CREEP AND FRACTURE BEHAVIOUR OF LEAD-CONTAMINATED ALUMINIUM ALLOYS OF 6000 SERIES

J. Aegerter[1)], M. Schaper[2)]
[1)] Hydro Aluminium Deutschland GmbH, Georg-von-Boeselager-Straße 21, D-53117 Bonn, Germany
[2)] Institut für Werkstoffwissenschaft, TU Dresden, Helmholtzstraße 7, D-01062 Dresden, Germany

ABSTRACT

Based on previous failure cases of lead-contaminated aluminium alloys of the 6000 series, the influence of lead on the creep and fracture behaviour of alloy EN AW-6082 was investigated. Typical creep data for notched and unnotched specimens were acquired for variants of the base alloy, each with different lead concentrations lower than the specification limit of 500 ppm. Time to fracture, the Norton exponent and activation energy were determined to highlight the embrittling effect of Pb under creep conditions. Fractographic investigations using light microscopy and scanning electron microscopy revealed an increasing percentage of intergranular fracture in those variants with higher lead concentrations specifically at low loads (longer loading times). An explanation regarding the mechanism of the time-dependent embrittlement of alloys containing small amounts of lead will be given, along with recommendations on how to prevent cases of this type of damage.

KEYWORDS

EN AW-6082, creep behaviour, delayed brittle fracture, lead contamination

INTRODUCTION

In the past, several cases of damage in aluminium forgings and extrusions of the 6000 alloy series were investigated. All of these investigations (e.g. [1]) showed that high lead concentrations could be observed in the damaged forgings or extrusions.
The harmful effect of Pb on the life time of alloys nearly the type EN AW-6060/6063 (formerly known as AlMgSi0.5) to fracture at elevated temperatures (i.e. 100°C) was described in [2]. The underlying mechanism was characterised as a form of "solid metal-induced embrittlement" in [3]. It is suggested that, under long-term tensile stresses, low melting in the matrix insoluble and precipitated elements (so-called "embrittlers") at grain boundaries may lead to the weakening of grain boundaries due to penetration already at temperatures below their melting point. The thickness of these low-melting metal films is expected to be only one or a few atom layers.
The present results of some recent investigations into creep behaviour are given in this paper. Further investigations are carried on in order to gain more knowledge and improved understanding of these effects.

MATERIALS AND INVESTIGATIONS

Manufacture of the test material

On the basis of a master alloy (EN AW-6062), variants with different Pb contents (see Table 1) were manufactured using the classical route: DC casting – homogenisation – extrusion – heat treatment. The processing parameters are listed in Table 2. It should be noted that the variants A, C and D were manufactured in one campaign; variant E (0.49 mass % Pb) was produced subsequently and in respect of better detectability of Pb. Therefore, the mechanical properties and the creep data of variant E were not fully available in the following, and the comparability is not 100 %.

No.	Si	Fe	Cu	Mn	Mg	Cr	Ni	Zn	Ti	Ga	Pb
EN AW-6082	0.7 - 1.3	0.5	0.1	0.4 - 1.0	0.6 - 1.2	0.25		0.2	0.1		
	Others: each 0.05, total: 0.15										
A	1.18	0.36	0.048	0.78	0.96	0.027	0.0013	0.048	0.023	0.0106	0.0029
C	1.09	0.33	0.039	0.71	0.99	0.027	0.0011	0.041	0.024	0.0108	0.0265
D	1.14	0.33	0.045	0.71	1.00	0.031	0.0012	0.047	0.024	0.0107	0.0322
E	1.11	0.30	0.047	0.74	0.93	0.030	<0.001	0.046	0.024	0.0105	0.490

Table 1: Chemical composition of the test material in mass % (Method: S-OES)

Production step	**Parameters**
DC casting	Billet diameter: 143 mm
Homogenisation	12 h, 480°C
Extrusion	Direct, billet and billet holder temperature: 480°C, die: bar 70 mm × 20 mm
Heat treatment	Solution heat treatment: 530°C 1h MT in air furnace, water quenching Stretching: 1 % plastic strain Ageing: 16 h at 160°C

Table 2: Processing parameters of the EN AW-6062 alloy investigated

Mechanical properties and microstructure

With a view to determining the comparability of the mechanical properties and the quality of the heat treatment, tests were performed at room temperature and at 80°C in accordance with EN 10002-1 and EN 10002-5 (for results, see Table 3). The position of the test pieces and the testing direction are shown in Fig. 1 (Testing direction: transverse (T), parallel length centred in middle of the cross-section of the bar). The microstructures of the different alloy

variants display the typical non-recrystallised grain structure for the chosen processing route and no significant differences between the variants. Fig. 2 shows as an example the grain structure in a longitudinal section.

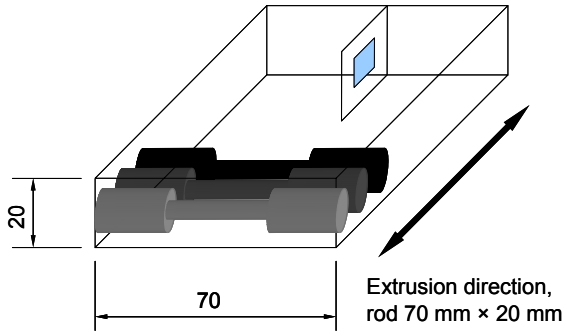

Fig. 1: Position and orientation of the specimens for tensile and creep tests with longitudinal metallographic section indicated

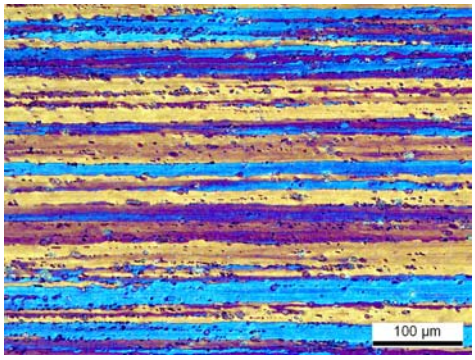

Fig. 2: Non-recrystallised grain structure (longitudinal cut, magnification 200:1, anodised, polarised light)

	Test temperature: RT (22°C ± 2°C)				Test temperature: 80°C			
Alloy variant	$R_{p0.2}$ [MPa]	R_m [MPa]	A [%]	Z [%]	$R_{p0.2}$ [MPa]	R_m [MPa]	A [%]	Z [%]
A	332	352	12.2	29	304	322	15.2	39
C	324	345	14.6	28	299	317	14.0	31
D	327	347	13.1	27	303	321	14.4	34
E	336	360	12.4	24				

Table 3: Tensile properties of the test material at room temperature and 80°C, test direction: T (transverse, see Fig. 1)

CREEP TESTS

Creep tests on notched test pieces

Creep tests on notched test pieces (stress concentration factor k_t = 4.5 [4, 5], d_n = 6 mm) were performed at room temperature (22°C ± 1.5°C) and at 80°C. The chosen test direction was transverse (T) to the extrusion direction; this means that the notch – and therefore the fracture direction – is parallel to the stretched microstructure and to the grain boundaries respectively. (In previous investigations, this direction was identified as being more sensitive to embrittlement than the longitudinal one.) The results of the tests on the notched test pieces are shown in Fig. 3 and 4.

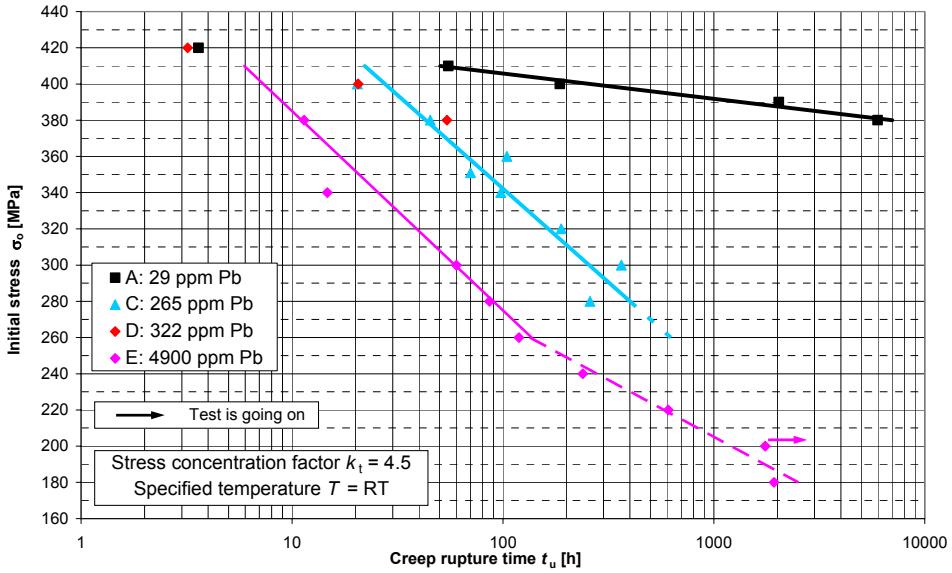

Fig. 3: Stress / creep rupture time diagram for notched test pieces at room temperature

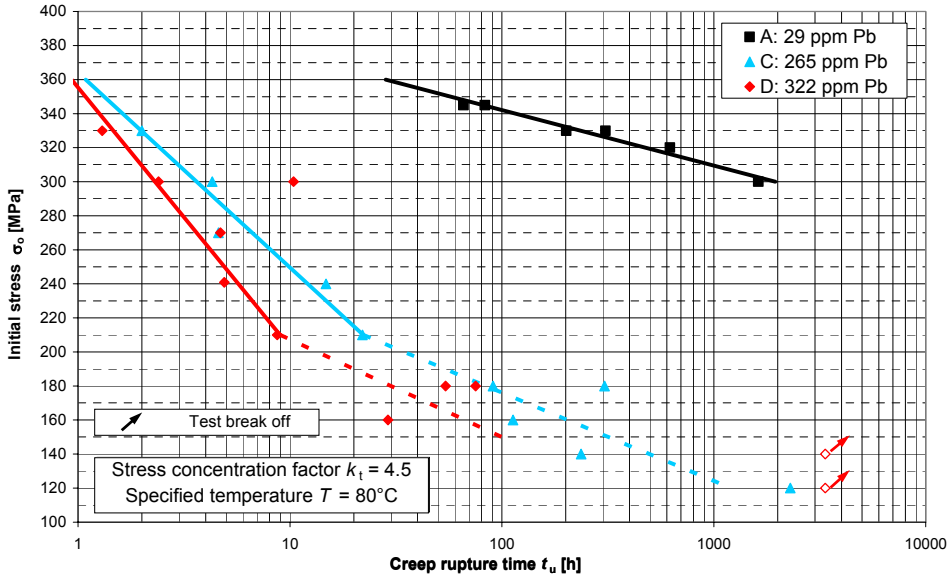

Fig. 4: Stress / creep rupture time diagram for notched test pieces at 80°C

Creep tests on unnotched test pieces

Creep tests were performed on unnotched test pieces (d_o = 5 mm) at 80°C, 120°C and, in part, at 100°C in accordance with EN 10291 [4] under constant load. During the test (including the loading phase), the elongation and – for documentation purposes – the temperature of the test piece were measured continuously and stored by means of a computer-controlled data acquisition system. The percentage elongation after creep rupture A_u and the percentage reduction of area after creep rupture Z_u were determined after the test by measuring the necessary input data directly from the test piece. The creep rupture time t_u was indicated directly by the testing device. Selected results of the tests are given in Fig. 5 and 6.

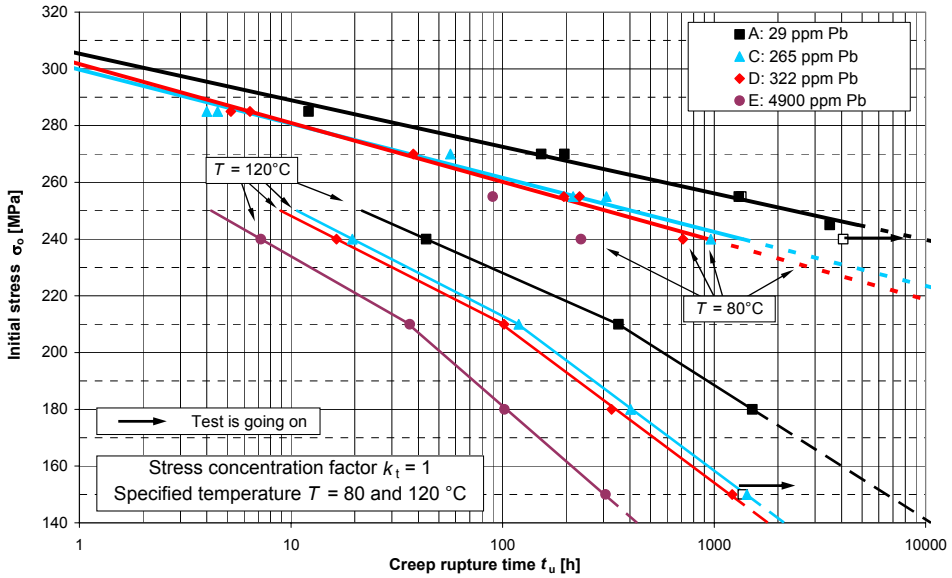

Fig. 5: Stress / creep rupture time diagram: T = 80 and 120°C, non-notched test pieces

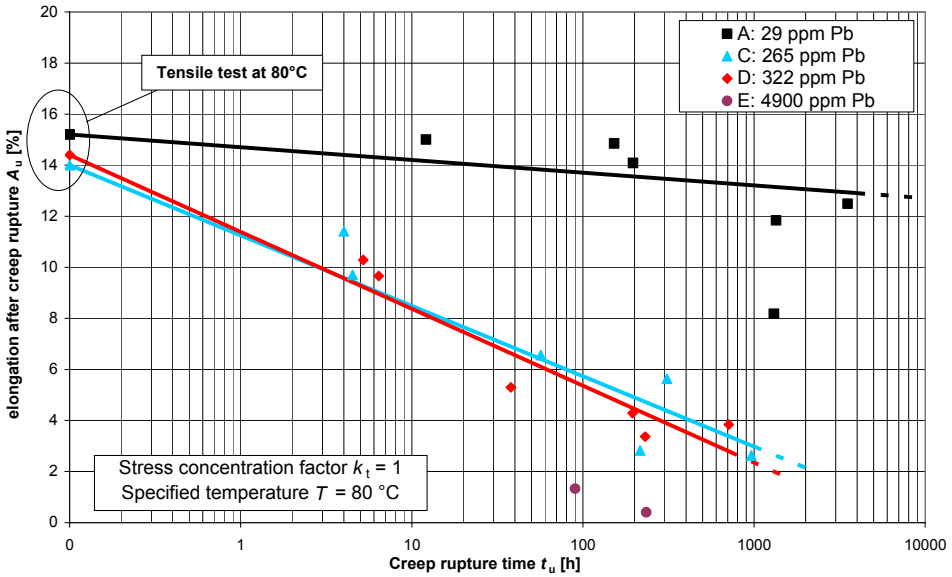

Fig. 6: Creep rupture deformation diagram: Increasing deterioration of elongation at rupture with higher lead content

Evaluation of the data from creep tests on unnotched test pieces

The elastic elongation, plastic elongation and minimum creep rate were calculated using the stored elongation time data and by making correlations to the stress steps during loading (i.e. from the weights used). In respect to the very small plastic elongation (≤ 1 %), where minimum creep rates were observed, the transformation to true stress and true strain respectively with regard to the true strain rate was unnecessary.

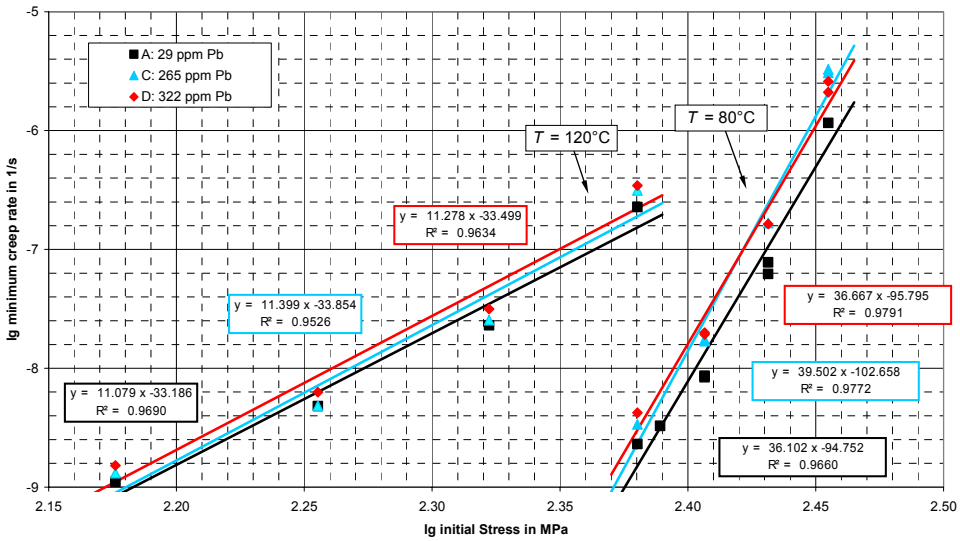

Fig. 7: Norton plot of minimum creep rate versus stress with regression analysis for the determination of the Norton exponent

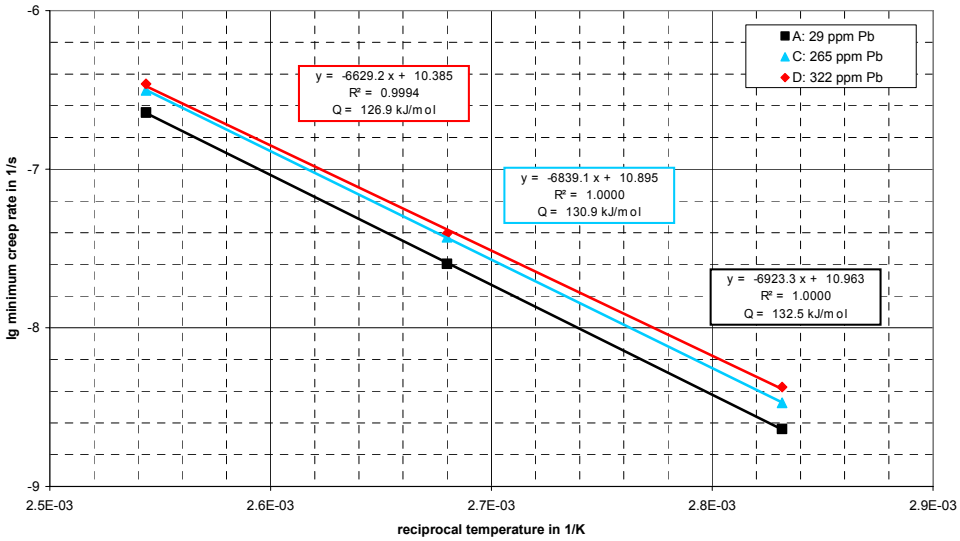

Fig. 8: Arrhenius plot of minimum creep rate versus reciprocal temperature with regression analysis for the determination of the activation energy, initial stress σ_o = 240 MPa

Fractographic investigations (light-microscopy and scanning electron microscopy)

The fracture surfaces of the broken creep test pieces were investigated using a stereo-light-microscope and a scanning electron microscope (SEM). Fig. 9a – 9c show a selection of SEM photos which give an overview of the different fracture structures depending on the Pb content of the respective alloy variant.

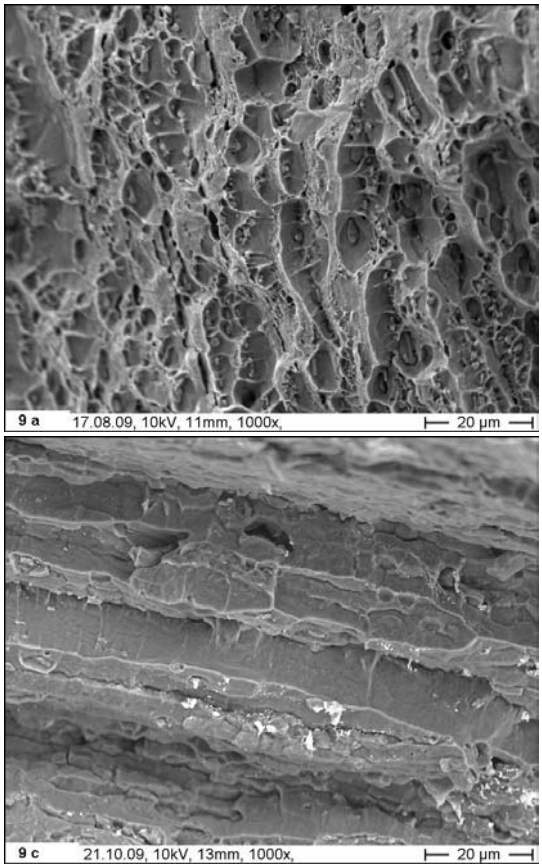

Fig. 9a – 9c: Fracture surfaces of broken test pieces after creep test: 9a: Variant A with 29 ppm Pb, Variant D with 322 ppm Pb, Variant E with 4900 ppm Pb

DISCUSSION OF THE RESULTS AND COMPARISON WITH LITERATURE DATA

The results of the creep tests on the notched test pieces show that a dramatic decrease in creep-rupture-time occurs due to increased Pb-concentration - even when this concentration remains below the specification limit of 500 ppm - at elevated and at ambient temperatures (see Fig. 3 and 4). The decrease at lower initial stresses – and therefore at longer loading times – is significantly higher. It can also be observed through a noticeable flattening of the curves that a threshold stress value [3] seems required for the reduced lifetime of variants containing Pb. The reduced lifetimes of the variants due to their Pb content were also observed in the creep tests on the unnotched test pieces (Fig. 5). The ductility properties of the variants (elongation after creep rupture A_u (Fig. 6) and reduction of area after creep rupture Z_u [1]) were also seen to decrease dramatically with longer lifetimes and increased Pb content. This correlates with the increase in the percentage of intergranular fracture at higher lead concentrations [2, 3] and lower load levels (longer loading times), see Fig. 9a – 9c.

The evaluation of the minimum creep rates depending on the initial stress (Fig 6, Norton law) shows very high stress exponents ($n \approx 36$ for $T = 80°C$, $n \approx 11$ for $T = 120°C$) nearly independent of the Pb content. It seems that the minimum creep rate increases with increasing Pb content. One explanation for this could be that the elongation measurements performed in the creep test is an integral measurement across the grains and grain boundaries. Assuming that the harmful effect of Pb is concentrated at the grain boundaries, the weakening of the grain boundaries leads to higher local elongations (over the grain boundaries) and to a higher – integral – elongation per time unit (i.e. creep rate).

Fig. 6 also shows that the use of Norton's law for these alloy/temperatures/stresses does not result in the best fit. An exponential function or sinh-function [6] gives a better approximation. According to [6], values of approximately $n \approx 3$ for monophase alloys, $n \approx 4$ to 5 for pure metals and values for n up to 40 for multiphase alloys can be found. Values greater than 20 should be typical for high stress levels and for the transition from creep to plastic deformation [7].

The evaluation of the activation energy (Fig. 7) gave values of between $Q_{(322\ ppm\ Pb)}$ = 126.9 kJ/mol and $Q_{(29\ ppm\ Pb)}$ = 132.5 kJ/mol. This marginally reduced activation energy for higher Pb-contents has to be confirmed by carrying out additional tests, e.g. by tests on alloy variant E (4900 ppm Pb) and/or tests at another initial stress.

In general, the values in our tests are comparable with those found in the literature: 114.7 kJ/mol [8], 142 to 150 kJ/mol (depending on the stress level) [7] and 142kJ/mol for the self-diffusion of pure aluminium [9].

RECOMMENDATIONS FOR THE PREVENTION OF SIMILAR CASES OF DAMAGE

The main basis for the prevention of similar cases of damage is a good understanding of the mechanism at work. In literature [3], the mechanism of solid metal induced embrittlement (SMIE) is shown to be analogous to liquid metal embrittlement (LME). According to the results of the investigations mentioned above and reported in the literature as well as from our failure experience a critical combination of tensile stresses, long term loading at enhanced temperatures and grain boundary enrichments of low-melting insoluble species represents the prerequisite of SMIE as shown in Fig. 10 (Fig. motivated by [10]).

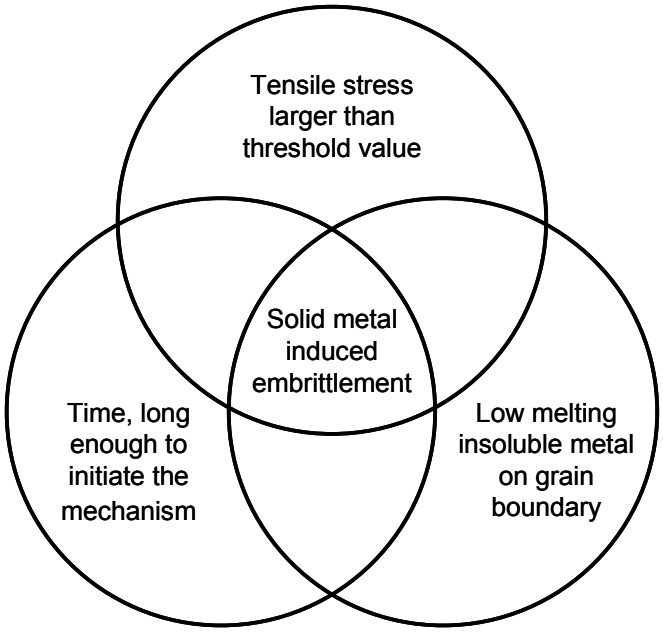

Fig. 10: The three basic parameters for SMIE

Obviously, the stressing time in normal tensile tests is too short to initiate SMIE. This means that normal (short-term) component testing will not give an answer to durability. In case of doubt, long-term material testing is necessary. The second main parameter is the exposure to tensile stresses, whereby a threshold value must be exceeded. The third parameter is the

presence of a low melting insoluble metal, which concentrates and distributes at the grain boundaries). According to the existing standards, for many alloys the maximum allowed content of such elements is 500 ppm. As shown by our investigations this limit is far too high - this could represent a big danger in the remelting of scrap from unknown sources. A reduction in the prescribed maximum concentration of embrittler species, therefore, seems to be required. On the other hand the dangerous consequences of such embrittling elements might be reduced/avoided by removing them in the form of intermetallic phases, by increasing the overall grain boundary surfaces in fine grained material or by choosing/setting up the main stress axis of the component parallel to the stretched microstructure.

REFERENCES

[1] Aegerter, J.; Finkelnburg, W.-D.; Schaper, M.:
Zeitstandverhalten von Schmiedeteilen aus der Legierung AlSi1MgMn (AA6082)
(Creep behaviour of AlMn1MgMn (AA6082) forgings)
MP Materials Testing, Vol. 51, (2009) 11-12, page 783 – 787
(also contained in: Conference script "Werkstoffprüfung 2008", DVM 2008, ISBN 978-3-00-026399-6, page 237 – 244)

[2] Guttmann, M; Quantin, B.; Dumoulin, Ph.:
Intergranular creep embrittlement by non-soluble impurity: Pb in precipitation hardened Al-Mg-Si alloys
Metal Science, Vol. 17, March 1983, page 123 - 140

[3] Kim. Y. S.:
Solid Metal-Induced Embrittlement of Metals and Alloys
RIST Journal of Research & Development. Vol. 17 No. 1 (2003)

[4] DIN EN I0291:(01-2001): Metallische Werkstoffe – einachsiger Zeitstandversuch unter Zugbeanspruchung – Prüfverfahren, Beuth-Verlag, Berlin

[5] Beiblatt 1 zu DIN EN I0291:(01-2001): Metallische Werkstoffe – einachsiger Zeitstandversuch unter Zugbeanspruchung – Prüfverfahren, Beuth-Verlag, Berlin

[6] Bürgel, R.:
Handbuch Hochtemperatur-Werkstofftechnik
Vieweg-Verlag, 3. reprint, Dec. 2006, ISBN 978-3-528-23107-1, page 97 ff.

[7] Minichmayr, R.; Riedler, M.; Eichlseder, W.:
Evaluation of creep behaviour and fatigue life under TMF-loading for alloy AlCuBiPb
11th International Conference on Fracture, (ICF11), Turin (Italy), March 2005

[8] Jaffe, N.; Dorn, J. E.:
Effect of temperature on the creep of polycrystalline aluminium by the cross-slip mechanism,
University of California, Materials Central, Contract No. AF 33(616)-3860, Project No. 7360, June 1960

[9] Gandhi, C.; Ashby, M. F.;
Fracture-mechanism maps for materials which cleave: FCC
BCC and HCP metals and ceramics", Acta Metall., 27, 1979

[10] Pohl, M.; Luithle, A.:
Flüssigmetall induzierte Spannungsrisskorrosion – Schadensmechanismen und ihre Auswirkungen
Conference script "Werkstoffprüfung 2007", Verlag Stahleisen GmbH, Düsseldorf 2007, ISBN 978-3-514-00753-6, page 25 - 34

Corresponding author: johannes.aegerter@hydro.com